

12.1 A Diverse Selection of Organelle Probes

Molecular Probes offers a diverse array of cell-permeant fluorescent stains that selectively associate with the mitochondria, lysosomes, endoplasmic reticulum and Golgi apparatus in live cells, including our exclusive MitoTracker, MitoFluor, LysoTracker, LysoSensor, RedoxSensor and ER-Tracker organelle stains (Figure 12.1). These probes, which are compatible with most fluorescence instrumentation, provide researchers with powerful tools for investigating respiration, mitosis, apoptosis, multidrug resistance, substrate degradation and detoxification, intracellular transport and sorting and more. Moreover, unlike antibodies, these fluorescent probes can be used to investigate organelle structure and activity in live cells with minimal disruption of cellular function (Figure 12.2). A particularly useful application of our live-cell organelle stains is to demonstrate the colocalization of green-fluorescent protein (GFP) expression and selective organelle staining by our red-fluorescent organelle stains.¹⁻⁴ An excellent compendium of human diseases that affect intracellular transport processes through lysosomes, Golgi and endoplasmic reticulum (ER) has been published.⁵

We have also introduced a large collection of organelle-specific monoclonal antibodies for both mammalian and yeast cells that can be used for immunolocalization, immunoprecipitation and Western blot analysis. Our antibodies to mitochondrial proteins (Section 12.2, Table 12.3, Table 12.5, Figure 12.31) provide a unique set of tools for understanding the assembly and function of the mitochondria. Cell-permeant and -impermeant fluorescent stains for the nucleus are described in Chapter 8, probes for the cytoskeleton in Chapter 11, and plasma membrane stains in Chapter 13. A variety of probes for phagocytosis, endosomes and lysosomes — including membrane markers as well as ligands for studying receptor-mediated endocytosis — are discussed in Section 16.1.

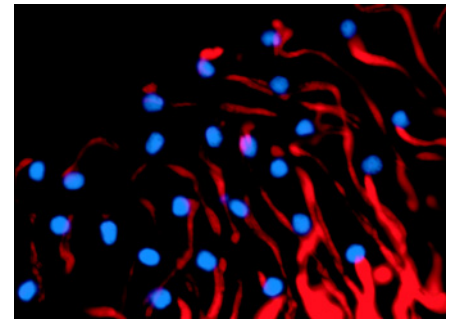


Figure 12.2 Euphyre spermatozoa from the pupal testis of the gypsy moth (*Lymantria dispar*) that were incubated in a solution of MitoTracker Red CMXRos (M-7512). The sample was subsequently fixed and the nuclear material was counterstained with the blue-fluorescent dsDNA dye, DAPI (D-1306, D-3571, D-21490). Image contributed by Laura K. Garvey, Department of Molecular and Cell Biology, University of Connecticut.

References

1. Mol Biol Cell 11, 1789 (2000);
2. J Biol Chem 274, 37233 (1999);
3. Biochem Biophys Res Commun 242, 390 (1998);
4. J Biol Chem 272, 14817 (1997);
5. Traffic 1, 836 (2000).

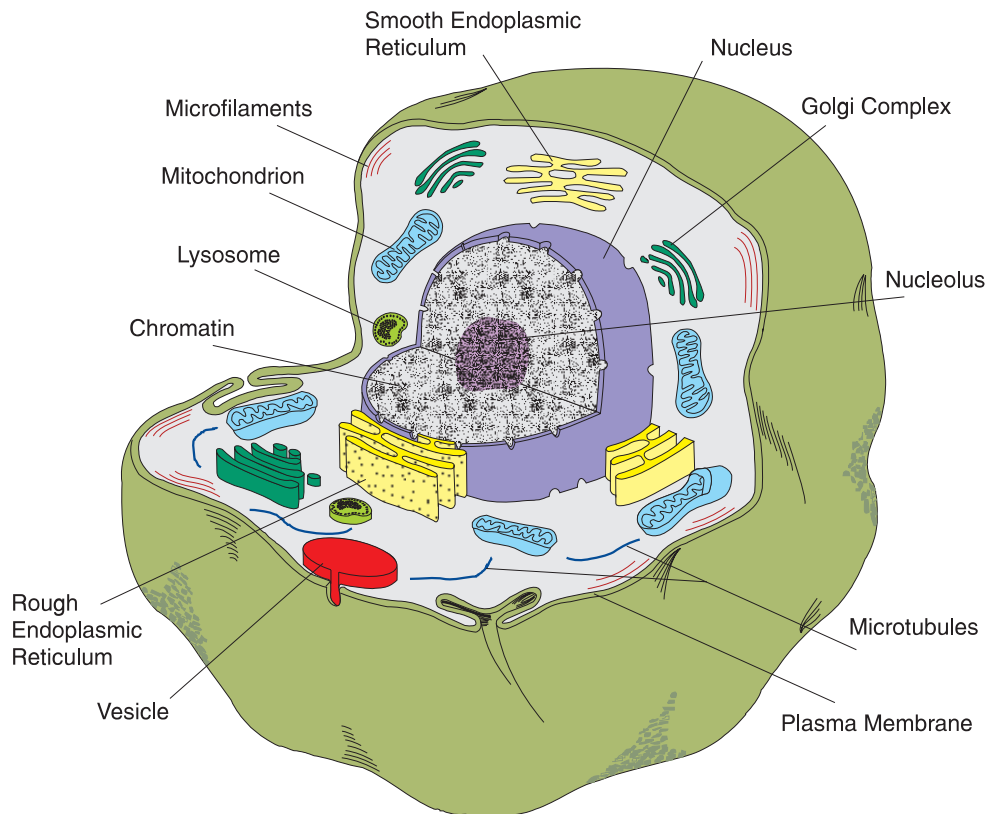


Figure 12.1 An animal cell.

TECHNICAL NOTE

Wide-Field Deconvolution Microscopy

Wide-field deconvolution microscopy consists of a tripartite system: a conventional fluorescence microscope equipped with a movable z-axis stage that permits imaging of the specimen at different focus positions, a CCD camera for quantification of the light emitted by the specimen, and a software package that is capable of correcting for distortions and information loss inherent in the imaging process.

A dominant characteristic of images collected with a wide-field fluorescence microscope is that at some level the image becomes blurred. Blurring can come from two sources: 1) contributions of out-of-focus light to the imaging plane and 2) diffraction. Large scale blurring is the result of light that is reflected and/or emitted from objects above and below the focal plane. These contributions blur the in-focus object; generally the farther away the contribution is from the in-focus plane, the more blurred the image becomes. Diffraction is a result of the interaction of light with matter — the tendency of light waves to “bend” when they pass an obstacle. Even if an imaging system is perfectly focused, diffraction effects that make it hard to discern details finer than roughly half the wavelength of the incident light. In the visible spectrum, the diffraction limit restricts resolution of objects smaller than ~200 nm (for blue light) to ~350 nm (for red light). Since many biologically interesting structures are smaller than 200 nm, the diffraction limit poses a serious limitation for optical microscopy.

Image restoration, or deconvolution strives to correct these problems. When applied to wide-field data, deconvolution can significantly reduce blur contributions, resulting in increased resolution and greatly improved contrast¹ (Figure 1, Figure 2). Other types of microscopy may also benefit from deconvolution: confocal laser-scanning microscopy,² two-photon microscopy,² and 4Pi microscopy.³ The combination of 4Pi microscopy and deconvolution is currently the pinnacle of optical resolution, allowing for resolution of objects at or below the diffraction limit.^{4,5}

The mathematical algorithms for deconvolution take a variety of forms. The earliest algorithms, developed in the mid-1980s⁶ employed techniques where the blur in each plane was suppressed by subtracting blurred versions of its “nearest neighbors.” However,

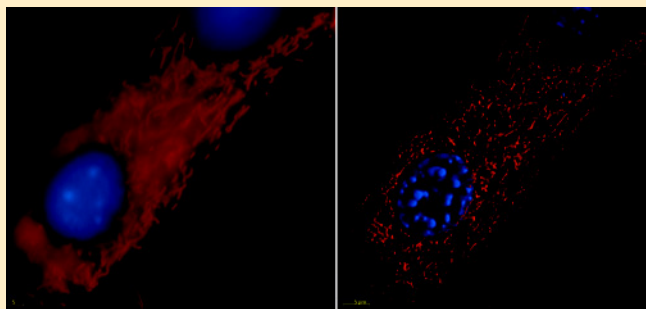


Figure 1 Bovine pulmonary artery endothelial cells were incubated with MitoTracker Red 580 (M-22425) to label the mitochondria. After fixation, the cells were counterstained with DAPI (D-1306, D-3571, D-21490) to label the nucleus. The panels show the unprocessed image (left panel), and after deconvolution (right panel). The image was deconvolved using Huygens software (Scientific Volume Imaging, www.svi.nl). 3-D reconstruction was performed using Imaris software (Bitplane AG).

modern computing power has allowed far more sophisticated algorithms to become practical. For example, the fast maximum likelihood estimate (MLE) algorithm considers the light contributions made to that location by all other points within the measurement space. Doing so results in reassignment of the out-of-focus light back to the original source from which it has been estimated to have come. To improve accuracy, such algorithms function iteratively, refining the estimate of the true object in a step-by-step fashion.

Although requiring significant computing power, image deconvolution in conjunction with standard fluorescence imaging can provide significant improvements to the scientific value and quality of the images collected. Deconvolved images in this *Handbook*, on our Web site and in other publications make use of Huygens software (Scientific Volume Imaging), which utilizes an accelerated MLE algorithm. This software may be used for processing of time-resolved two- and three-dimensional multichannel images from wide-field, confocal, scanning disk confocal, two-photon and 4Pi microscopes. In all publications, we indicate in the picture captions when we have used deconvolution techniques to improve the resolution of the picture. Additional examples of pictures in which we have used image deconvolution include Figure 11.4, Figure 12.5 and Figure 12.36.

References

1. *J Opt Soc Am A* 8, 893 (1991);
2. *Bioimaging* 4, 187 (1996);
3. *J Microsc* 187, 1 (1997);
4. *Ultramicroscopy* 87, 155 (2001);
5. *J Struct Biol* 123, 236 (1998);
6. *Methods Cell Biol* 30, 353 (1989).

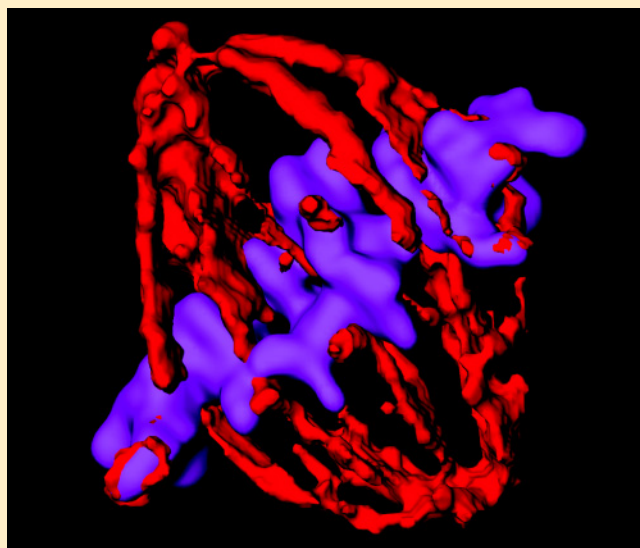


Figure 2 Expanded view of the nuclear region of a metaphase muntjac skin fibroblast showing tubulin and chromosomal structure. Tubulin was stained with an anti- α -tubulin antibody (A-11126), pre-labeled with the Zenon One Alexa Fluor 568 Labeling Kit (Z-25006) and chromosomes were stained with an anti-cdc6 peptide antibody (A-21286) pre-labeled with the Zenon One Alexa Fluor 647 Labeling Kit (Z-25008). The image was deconvolved using Huygens software (Scientific Volume Imaging, www.svi.nl). 3-D reconstruction was performed using Imaris software (Bitplane AG).